Evaluation of MRR in ECDM Process with FEA

Dilpreet Singh[1], Mudimallana Goud[2]

[1]M.Tech, Dept. of Production and industrial engineering, Punjab Engineering College, Chandigarh, India

[2]Associate Professor, Dept. of Production and industrial engineering, Punjab Engineering College, Chandigarh, India

---***---

Abstract - *Electro chemical discharge machining (ECDM) or Electro chemical spark machining (ECSM) or Electrochemical anode machining (ECAM) or Spark assisted chemical machining (SACM) is one of the non-conventional machining process. This process is predominantly used for machining electrically non conducting materials. ECDM is a hybrid process combination of both Electrical discharge machining (EDM) and Electro-chemical machining (ECM) the electrical discharge during machining results in major material removal while the chemical action results in minute material removal which helps in obtaining better surface finish. An attempt has been made to develop a finite element simulation model to evaluate material removal rate (MRR) in case of quart and the results are compared with the experimental results available to validate the model.*

*Key Words***:** Electro chemical discharge machining, finite element analysis, material removal rate, heat transfer, Gaussian function

1. INTRODUCTION

Electro chemical discharge machining (ECDM) or Electro chemical spark machining (ECSM) or Electrochemical anode machining (ECAM) or Spark assisted chemical machining (SACM) is one of the non-conventional machining process. This process is predominantly used for machining electrically non conducting materials. ECDM is a hybrid process combination of both Electrical discharge machining (EDM) and Electro-chemical machining (ECM) the electrical discharge during machining results in major material removal while the chemical action results in minute material removal which helps in obtaining better surface finish. This process was first reported in 1968 and since then lot of research has been done to develop this process and this research is still going on till the present day to increase its industrial and commercial viability. ECDM involves the complex phenomenon of spark discharge whose mechanism is still not completely explained. One of the most positive point about this type of machining is that it can easily cut hard to machine and high hardness material easily. Tool wear during machining is also minimal as tool never really comes in contact with the workpiece. As the voltage is applied across the gap between the electrode and the workpiece the formation of bubbles initiates near the tip of the work piece and as the voltage applied increases a constant bubble film is formed near tool tip and as the voltage is further increased the voltage becomes just enough to create a spark discharge in the vapour region and thus

increasing the local temperature instantaneously and thus causing the material on the workpiece to melt and vaporise. The voltage at which the spark discharge takes place is called the critical voltage and this voltage is dependent on several other parameters. This complex phenomenon involves several input parameters such as applied voltage, inter electrode gap, type of electrolyte used, concentration of electrolyte used, electrode material, workpiece material, feed rate, current etc. Various output parameters of the interest are mostly Material removal rate (MMR), Surface roughness, form accuracy, heat affected zones etc. several authors have tried to correlate various parameters to increase the process capability. ECDM is mostly used in producing microchannel, micro holes and engraving on hard to machine materials. One of the reasons why the ECDM process is still not used in industry is because it is still under developmental phase and lot of work is still needed to be done to make this refine this process and make it more efficient.

Although the sparking phenomenon is not fully understood many attempts have been made by several authors. Basak and Ghosh [1] attempted to develop a theoretical model for spark discharge phenomenon they considered it kind of a switching phenomenon and considered inductance of the circuit as an important parameter. Bhattacharyya et al. [2] studied various process parameters that influence the material removal rate (MRR) such as voltage and electrolyte concentration they also studied various tool shapes that influence the generation of spark and found that a flat tip with some taper gives the stable arc. Jain and Chak [3] attempted to perform trepanning on alumina and glass with ECDM and reported a decrease in MRR with an increase in depth. Jain and Priyadarshini [4] investigated the machining of the microchannel in quartz and studied the influence of voltage on, the width, depth and heat affected zones on microchannel and found that as the voltage increases the MRR increases the width of channel increases, the width of HAZ increases and depth becomes non-uniform. Nguyen et al. [5] studied the effect of electrolyte level and feed rate on spark generation and spark stability while machining quartz and found that low electrolyte level increases the thermal energy as the resistance to the spark decreases current increases. Jawalkar et al. [6] studied the effect of various parameters on MRR while machining optical glass. Paul and Hiremath [7] attempted to use mixed electrolyte and studied the effect of voltage and duty factor on MRR and found out that micro-feature generation is difficult with mixed electrolyte then with NaOH alone.

Several authors have tried to correlate different parameters to predict MRR using various tools such as finite element analysis [8], Taguchi [9], response surface [10], fuzzy logic [11] and artificial neural network [12] every tool gives result considering some of the assumptions and no theory is completely generalized and widely accepted till present. Bhondwe et al. [13] carried out FEA two-dimensional thermal analysis and predicted MRR and compared the results with the previous experimental work to validate the mathematical model. Wei et al. [14] gave the finite element model for discharge regime where most of the metal removal takes place Jain et al. [8] developed the relationship between thermal conductivity and electrolyte concentration and then developed their finite element model. Paul and Korah [15] simulated the finite element model for pulsed spark and compared its result with normal spark and compared their MRR and maximum temperatures. Goud and Sharma [16] developed a finite element thermal model considering heat generation in three-dimensional Gaussian spark region and predicted MRR on silica glass and alumina, these results were then compared with the result available from the experiment and found to be in agreement.

The focus of the present study is to develop a three-dimensional finite element thermal simulation model with convective heat transfer taken into account for different materials and compare the results with the already available experimental results. To carry out the analysis ANSYS workbench transient thermal module is used which utilizes mechanical APDL solver and whose results are largely acceptable.

The schematic diagram of ECDM is very similar to that of ECM as shown in **Fig-1** tool is made cathode and is immersed up to 1 mm into the electrolyte. The reactions taking place at cathode [2] and the anode are as follows.

$$2H_2O + 2e^- \rightarrow 2(OH)^- + H_2$$
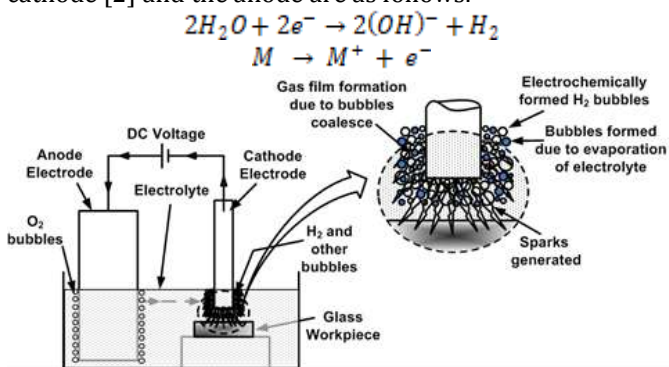$$M \rightarrow M^+ + e^-$$

Fig- 1: Schematic of basic ECDM machine showing important components (Goud and Sharma 2017)

At the time of spark discharge, most of the heat is lost in the evaporation of electrolyte in the form of latent heat of vaporization and some heat is lost to tool, very small amount of heat reaches the workpiece [1]. The peak temperatures produced during an electrical discharge are of the order of magnitude 10^4 so formation HAZ is likely to happen as reported by Yang et al. [18] they studied the effect of

wettability on gas film formation and reported that tungsten carbide tool has the lowest wear on its edge where the current density is considered maximum.

2. ASSUMPTIONS

For simplifying the finite element model following major assumptions are made.

- Material properties of materials are considered homogeneous and isotropic.
- Thermal conductivity and specific heat capacity are considered independent of temperature.
- Heat transfer due to radiation is neglected because the area over which high temperatures are observed is very small and thus nullifies the effect of high temperature.
- Heat transfer coefficient at the top surface of the workpiece is considered around 10000W/m2-K because at such high temperature the electrolyte will be boiling thus convective heat transfer falls in boiling regime.
- The spark region is considered to be of 150μm in radius and heat is supplied in single continuous spark.
- Only 20% of the total power supplied is considered to be going into the workpiece in the form of heat.
- Heat supplied to the spark region is considered to be a Gaussian function.
- The metal removal due to electrochemical action is not considered in this analysis.
- The formation of recast layers or resettlement of material is also neglected in this analysis

3. METHODOLOGY

For the purpose of analysis domain of the workpiece considered is of size 0.6x0.6x0.4mm of sample material which is immersed in the electrolyte and spark region is considered of about 300μm diameter. The distribution of heat over spark region is a Gaussian function.

$$f(x,y) = A e^{-\left(\frac{(x-x_0)^2}{2\sigma_x^2} + \frac{(y-y_0)^2}{2\sigma_y^2}\right)}$$

Here A represents the maximum amplitude and σ_x and σ_y represents the spread of the curve in our case both are assumed to be equal. The Gaussian equation used in the analysis is taken from Bhondwe et al. [13].

$$\dot{q} = \frac{4.5 E V_d I_d}{\pi R^2} exp\left\{-4.5\left[\left(\frac{r_x}{R}\right)^2 + \left(\frac{r_y}{R}\right)^2\right]\right\}$$

Here A represents the maximum amplitude and σ_x and σ_y represents the spread of the curve in our case both are assumed to be equal. The Gaussian equation used in the analysis is taken from Bhondwe et al. [13]. This equation is used to approximate the heat flux at the time of spark discharge. Here V_d represents the discharge voltage, I_d represents the discharge current and E represents the amount of power going in the form of heat to the workpiece

which is approximated around 20%. Voltage and current characteristics are derived from [1]. The graphical depiction of two dimensional Gaussian equation is shown in **Fig-2**. The Z axis here represents the heat flux $\dot{q}$ in W/m².
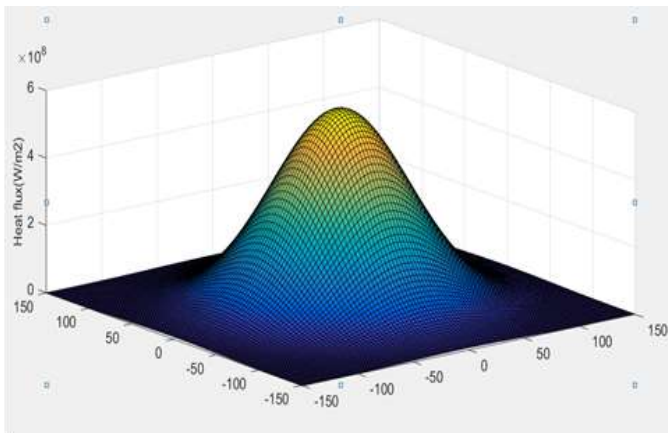

Fig-2: Gaussian distribution of heat flux

The thermal conduction equation is used as a governing equation to solve this problem.

$$\frac{\partial^2 T}{\partial x^2} + \frac{\partial^2 T}{\partial y^2} + \frac{\partial^2 T}{\partial z^2} = \frac{1}{\alpha}\frac{\partial T}{\partial t}$$

This equation is the transient thermal equation without heat generation here α represents the thermal diffusivity represented as the ratio of thermal conductivity to volumetric heat capacity. It determines how swiftly the heat can transfer through a material, higher the value of α faster the heat will transfer.

$$\alpha = \frac{k}{\rho c_p}$$

Where k is the thermal conductivity of workpiece is, ρ is the density of the material and c_p is specific heat capacity of a material.

	Quartz
Thermal conductivity(W/mK)	1.4
Spark radius(μm)	150
Fraction of energy transferred	0.2
Melting temperature(K)	1943
Initial temperature (K)	295
Convective coefficient (W/m²-K)	10000
Heat capacity(J/kg-K)	733
Density (kg/m³)	2650

Table-1: Values taken for analysis

3.1 Boundary conditions

Following boundary conditions and initial conditions are applied also shown in **Fig-3**.

1. The sidewalls and bottom surface are assumed to be adiabatic i.e.no heat transfer take place through these walls.

$$\frac{\partial T}{\partial x} = 0, \ \frac{\partial T}{\partial y} = 0, \ \frac{\partial T}{\partial z} = 0$$

2. The top surface is losing heat through convective heat transfer.

$$\dot{q}_c = h(T - T_0)$$

3. In the region of spark Gaussian heat flux is applied to the external load.
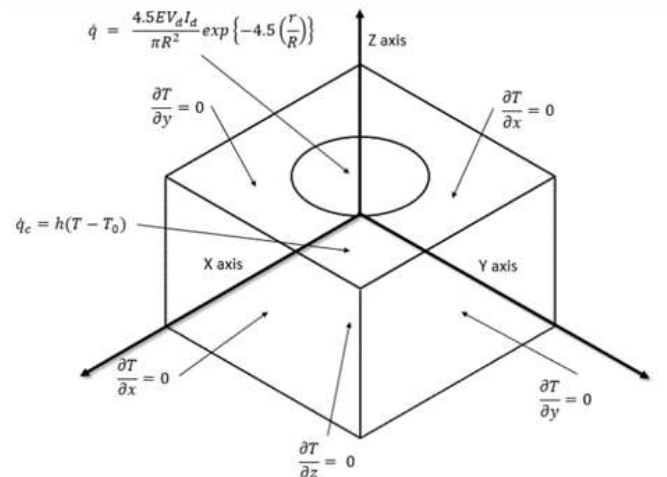4. The initial temperature of the workpiece and the surrounding is considered same 295K.

Fig-3: Boundary conditions applied to the workpiece

3.2 Meshing

Finite element analysis is performed in ANSYS 16 commercial package. For discretizing the domain ANSYS meshing tool is used. Tetrahedron elements are selected for meshing with patch conforming algorithm. This type of mesh is suitable for conduction heat transfer analysis. It can be seen in Figure 4 that the area where heat flux is applied is refined to capture results more accurately.

No. of Nodes.	No. of Elements.(e)	Maximum Temp. (K)	Mesh sensitivity $\Delta T/\Delta \varepsilon$
15120	10183	2091.6	-
28533	19619	2352	0.02759
65984	46441	2367	0.00055
111812	79446	2380	0.00042
216889	155681	2393	0.00017
353281	256305	2403	0.00010
501252	365900	2408	0.00004
1333557	**984251**	**2409.5**	**0.00000**

Table-2: Mesh sensitivity table

The **Table-2** shows that as the no. of elements and nodes keeps on increasing the difference between the temperature decreases and thus this point is considered as the best selection of no. of nodes. The data in the table is represented in graphical form in **Fig-6**.
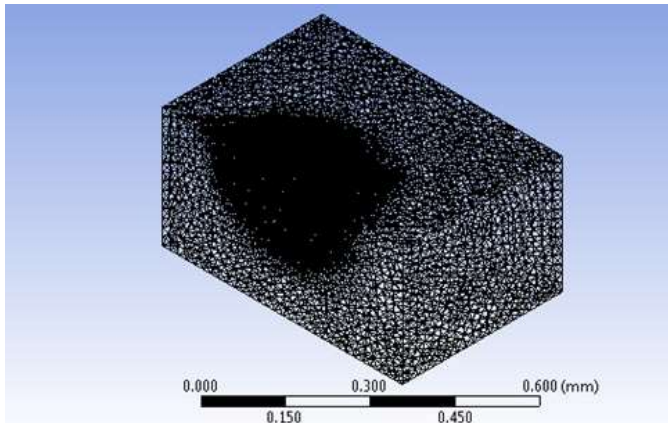
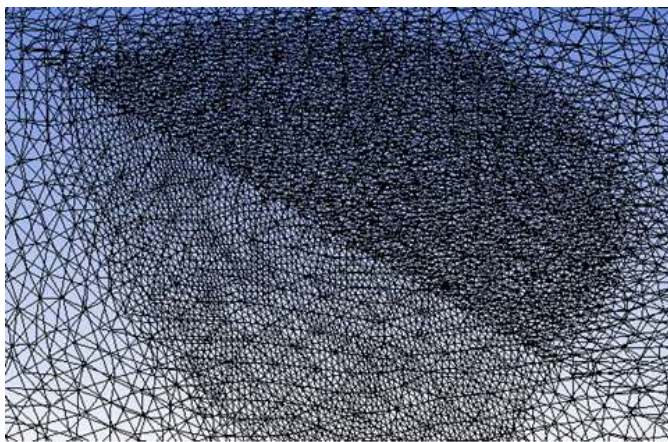**Fig-4:** Cross-section view of meshed workpiece refined at the spark region.

Fig-5: Detailed view of meshed workpiece refined at the spark region.

Refinement of the mesh is done only where the resolution of results is required or only in that area where the results are of interest.
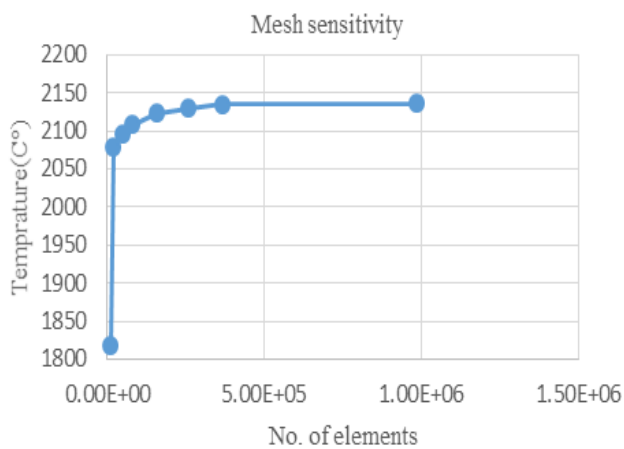

Fig-6: Variation of max. Temperature with no. of elements.

4. RESULTS AND DISCUSSIONS

The result of the analysis carried out show that very high temperatures exist at the centre of the spark and temperature gradients are also very high in this region. These high-temperature gradients are responsible for the formation of heat affected zones as reported by the author [4]. The temperature contour plot is shown in **Fig-7**.
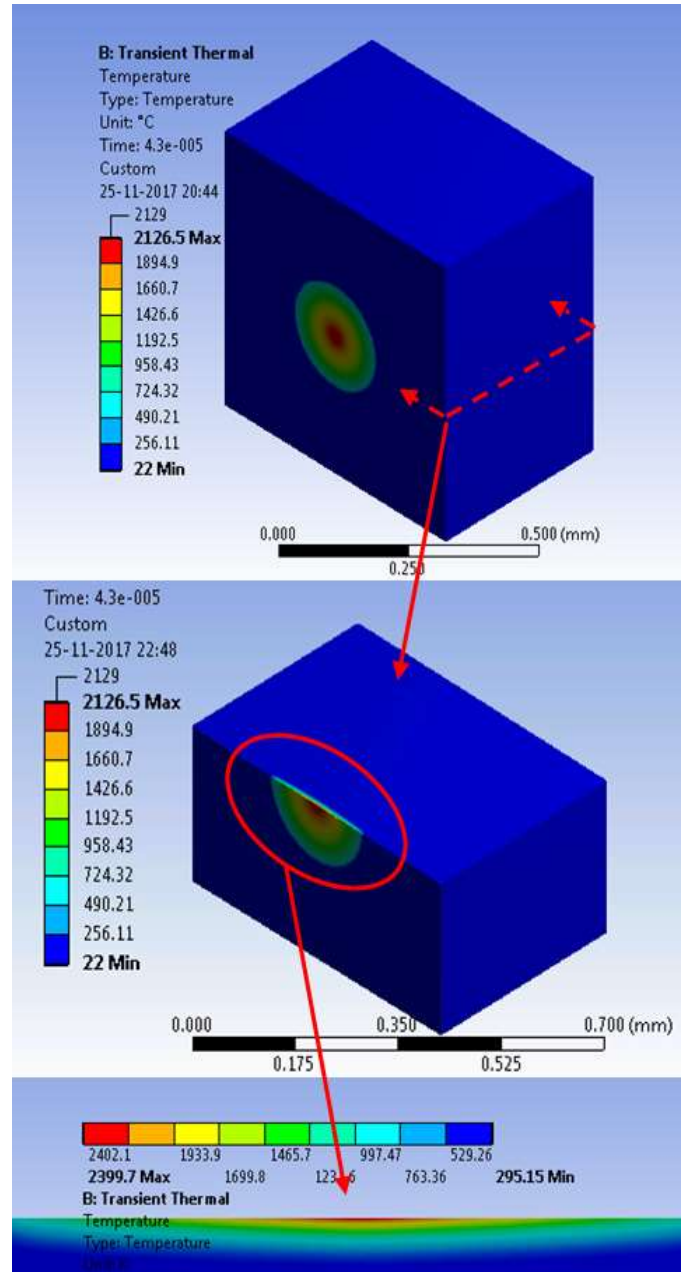

Fig-7 Temperature distribution obtained from the FEA thermal analysis for quartz material

For the calculation of the material removal rate contour plots are obtained with isotemperature curve. The melting point of material is noted down and an isotemperature curve is obtained for that material at melting point. This curve data is extracted from the ANSYS workbench and is fitted with a

polynomial curve. A sample calculation for finding material removal rate is being shown.

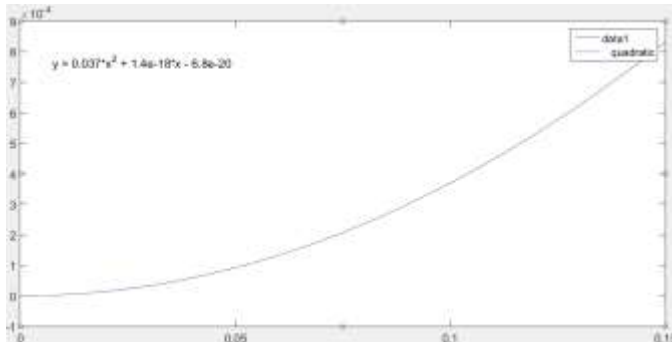Calculation performed for quartz material at 40 volts is shown.

Fig-8: Curve fitting on isotemperature data at melting point for quartz material at 40V from ANSYS

$$y = 0.037x^2$$

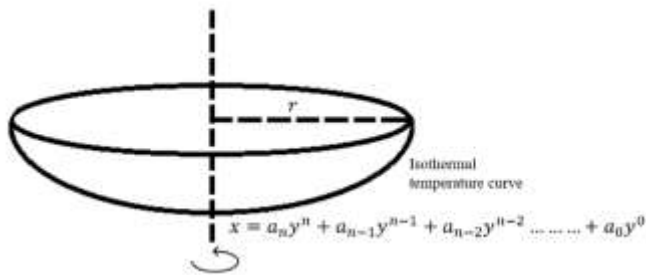Other terms are neglected because their value is very small and does not influence the final result.

Fig- 9: The volume of material removed using curve about a vertical axis

$$V = \int_0^r \pi x^2 dy$$

Here 0 to r represents the distance along y axis which in this case is from 0 to 0.00189mm and V represents the volume

$$V = \int_0^{0.00085} \pi \frac{y}{0.037} dy$$

$$V = 3.06 \times 10^{-5} \; mm^3$$

$$MRR = \frac{V\rho}{t_s}$$

(Here ρ is the density of material, t_s is the single spark time and V is volume)

$$MRR = \frac{3.06 \times 10^{-5} \times 2.65 \times 60}{2 \times 10^{-3}}$$
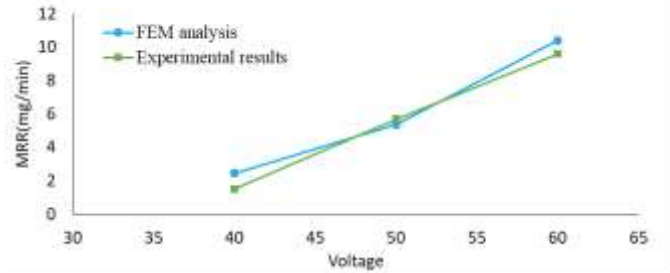
$$MRR = 2.46 \; mg/min$$

Fig-10: Comparison of MRR from FEA analysis with MRR from experimental results [4].

The effect of convective heat transfer is also studied with the help of simulation and results obtained are compared with experimental results and previous simulation results. The trend obtained in these results is similar to previous simulation results.

5. CONCLUSION

The simulation model presented for the calculation of MRR of quartz, soda lime glass and alumina agrees with the experimental observations. The high rate of increase of temperature and high thermal gradients confirm the formation of heat affected zones. The predicted MRR is less than the previous 3D simulation models because the effect of convection is considered in this model which results in higher heat loss to atmosphere and thus lower MRR. The other reason may be not considering the effect of a chemical reaction and thermodynamic instability in the model. The model also confirms that as the discharge voltage increases the maximum temperature also increases which results in an increase in MRR.

REFERENCES

[1] Basak I, Ghosh A. Mechanism of spark generation during electrochemical discharge machining: a theoretical model and experimental verification. J Mater Process Tech 1996; 62: 46-53.

[2] Bhattacharyya B, Doloi BN, Sorkhel SK. Experimental investigations into electrochemical discharge machining (ECDM) of non-conductive ceramic materials. J Mater Process Tech 1999; 95: 145–54.

[3] Jain VK, Chak SK. Electrochemical Spark Trepanning of Alumina and Quartz. Mach Sci Technol 2000; 4(2): 277-90.

[4] Jain VK, Priyadarshini D. Fabrication of Micro Channels in Ceramics (Quartz) Using Electrochemical Spark Micro Machining (ECSM). In: Proceedings of Global Engineering, Science and Technology Conference 3-4 October 2013, Bay View Hotel, Singapore.

[5]   Nguyen KH, Lee PA, Kim BH. Experimental Investigation of ECDM for Fabricating MicroStructures of Quartz. Int J Precis Eng Man 2015; 16 (1): 5-12.

[6]   Jawalkar CS, Kumar P, Sharma AK. Parametric study while micro channeling on optical glass using microcontroller driven ECDM process. Advanced Materials Research Vol. 585 (2012) pp 417-421

[7]   Lijo P, Hiremath SS. Characterisation of Micro Channels in Electrochemical Discharge Machining Process. Appl Mech Mater 2014; 490-491: 238–42.

[8]   V.K. Jain, P.M. Dixit, P.M. Pandey. On the analysis of the electrochemical spark machining process. International Journal of Machine Tools & Manufacture 39 (1999) 165–186.

[9]   Mitra NS, Doloi B, Bhattacharyya B. Analysis of Traveling Wire Electrochemical Discharge Machining of Hylam based Composites by Taguchi Method. International Journal of Research in Engineering & Technology 2014; 2(2): 223-36.

[10] Paul L, Hiremath SS. Response Surface Modelling of Micro Holes in Electrochemical Discharge Machining Process. Procedia Engineering 2013; 64: 1395–404.

[11] Skraalak G, Skrabalak MZ, Ruszaj A. Building of rules base for fuzzy-logic control of the ECDM process. J Mater Process Tech 2004; 149(1-3): 530–5.

[12] Sathisha N, Somashekhar S. Hiremath and Shivakumar J. prediction of material removal rate using regression analysis and artificial neural network of ecdm process, International Journal of Recent advances in Mechanical Engineering (IJMECH) May 2014; Vol.3, No.2

[13] Bhonwe KL, Yadava V and Kathiresan G. Finite element prediction of material removal rate due to electrochemical spark machining. Int J Mach Tool Manuf 2006; 46: 1699–1706.

[14] Chenjun Wei & Kaizhou Xu & Jun Ni & Adam John Brzezinski & Dejin Hu. A finite element based model for electrochemical discharge machining in discharge regime Int J Adv Manuf Technol (2011) 54:987–995

[15] Lijo Paul, Libin V Korah Effect of Power Source in ECDM Process with FEM Modeling. Procedia Technology 25 (2016) 1175 – 1181

[16] Goud M, Sharma A.K. A three-dimensional finite element simulation approach to analyze material removal in electrochemical discharge machining. Proceedings of the Institution of Mechanical Engineers, Part C: Journal of Mechanical Engineering Science 2016, 0954406216636167.

[17] Goud M, Sharma AK. On performance studies during micromachining of quartz glass using electrochemical discharge machining, Journal of Mechanical Science and Technology 31 (3) (2017) 1365~1372

[18] Yang CK, Cheng CP, Mai CC, Wang AC, Hung JC, Yan BH. Effect of surface roughness of tool electrode materials in ECDM performance. Int J Mach Tool Manu 2010; 50: 1088–96.